Vision Res. Vol. 27, No. 3, pp. 381–392, 1987
Printed in Great Britain.

0042-6989/87 $3.00 + 0.00

EXTRAOCULAR MUSCLE SIDESLIP AND ORBITAL GEOMETRY IN MONKEYS

JOEL M. MILLER and DAVID ROBINS
Smith-Kettlewell Eye Research Foundation, 2232 Webster Street, San Francisco, CA 94115, U.S.A.

(*Received* 8 *August* 1985; *in revised form* 24 *July* 1986)

Abstract—The belly of each extraocular muscle is elastically coupled to both the globe and orbit. The dependence of muscle planes on gaze angle must be determined experimentally. In monkeys, radio-opaque markers were implanted along the upper and lower margins of a lateral rectus. A scleral search coil was implanted in the other eye. With the eye in various gaze positions, X-ray images were made to show the LR in the lateral view. We found that as the eye rotates vertically over 50 deg (±25 deg), the point of tangency of the LR with the globe slips an average of 5.1 mm vertically with respect to the globe, allowing this point—and so the muscle plane—to remain approximately fixed relative to the orbit. The results of quantitative orbital dissections are presented in support of the sideslip calculations.

Extraocular muscle Monkey Muscle plane Muscle sideslip Ocular model Ocular statics Orbital geometry

INTRODUCTION

The first attempt at a complete analysis of the mechanics of binocular alignment (Robinson, 1975) became possible when human extraocular muscle force was first measured as a function of length and innervation (Robinson, 1969; Collins, 1969). Recently, it has been possible to improve on this model and extend it in a number of ways (Miller and Robinson, 1984). Some of the advances of this model (called "SQUINT") were:

(1) The theoretical analysis of muscle sideslip was improved. (This is further discussed below.)

(2) The distribution of force across the width of the muscle was treated, allowing the model to reflect the fact that as a muscle bends sideways (i.e. in the plane of its length and width) the point at which the distributed force may be thought to act (the effective insertion) moves toward the stretched edge.

(3) Translation of the eye in the orbit was treated. Translation is important both as an output variable (e.g. in certain disorders retraction is a diagnostic sign), and because of its influence on orbital geometry and, so, on eye rotation.

Of the data that would further refine and test the SQUINT model, we believe that measurements of muscle paths are the most important. The action of each muscle is considered as the product of a scalar muscle force F and a unit moment vector $\mathbf{m}$; F determines the magnitude of a muscle's effect on the eye, while $\mathbf{m}$ determines the direction of its pull ($\mathbf{m}$ is the axis about which a muscle tends to rotate the eye). While both must be known in a quantitatively correct model, if the $\mathbf{m}$ vectors are not known, the model will not even be qualitatively correct.

Each $\mathbf{m}$ vector is determined by the *origin* of the muscle, O, the *point of tangency* of the muscle with the globe, T, and the *center of rotation* of the globe, C (see Fig. 1).

Since the muscle is firmly attached to the globe only at the insertion, the point of tangency depends on the path taken by the muscle as it leaves the insertion. In primary position all of the muscles insert into the globe *beyond* the center of rotation. As the globe rotates to arbitrary positions, then, we expect the muscles to slip sideways with respect to the globe (see Fig. 1). The horizontal recti, for instance, should slip upwards as the eye elevates and downwards the eye depresses. If sideslip were unrestrained, a muscle would simply take the shortest path on the globe (a great circle) from insertion to point of tangency (Fig. 2). Early analyses by Krewson (1950) and Boeder (1962) assumed that this was the case. However, a complex arrangement of elastic connective tissue surrounds the muscles and couples them

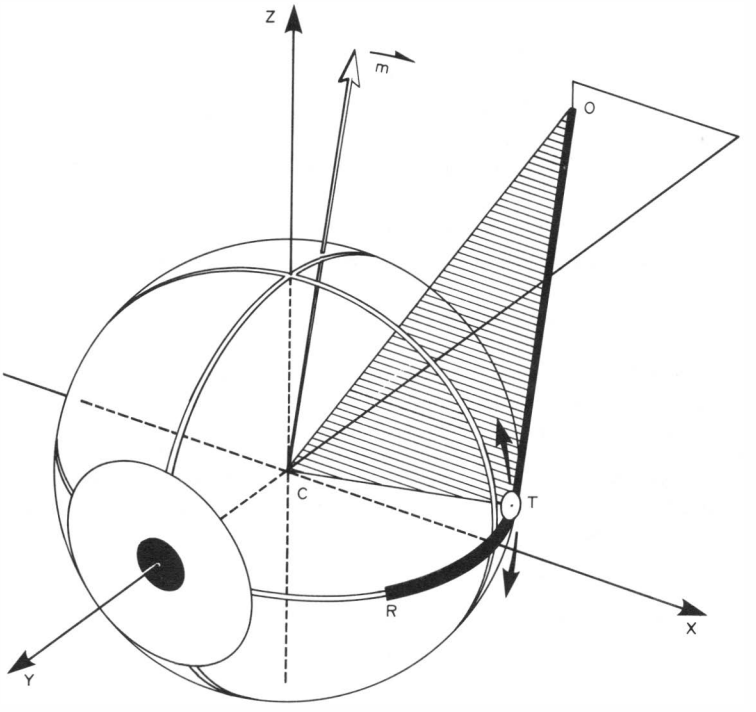

Fig. 1. Unit moment vector. A left eye in primary position is shown schematically, with only the lateral rectus muscle. A left-handed Cartesian coordinate system X–Y–Z is defined, with origin C at the center of rotation, X pointing laterally, and Y pointing straight ahead. The unit moment vector **m** is determined by the muscle origin O, the point of tangency T, and the center of rotation C. Sideslip, expected to occur as the eye rotates, would move T on the surface of the globe, as suggested by the arrows.

to each other and to the orbital walls (see Koornneef, 1983). We would expect globe-relative sideslip to be reduced by the heavy intermuscular membranes that form a sort of "cap" anterior to the equator of the globe.

Our model of muscle sideslip has previously been described in detail (Miller and Robinson, 1984). Briefly, we suppose the various fascial connections to the muscles act mainly as elastic attachments to the globe along the arc of con-

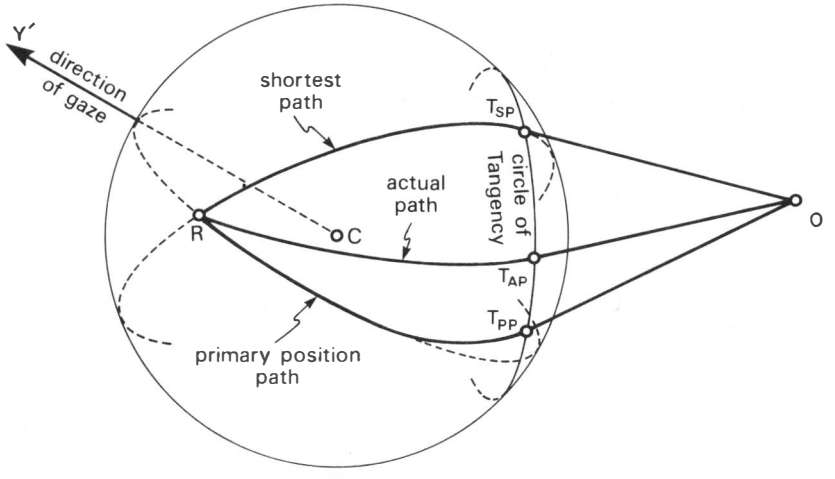

Fig. 2. Possible muscle paths. A lateral rectus is shown schematically, with the eye in elevation. We assume that the muscle's path from the origin O to the point of tangency T is a straight line. For any gaze position, then, we can then draw a "circle of tangency" on the globe. Because only R and O are fixed, T will fall at some unknown point on the circle of tangency. The "shortest path" (a great circle), would be taken by a muscle free to sideslip with respect to the globe without restraint; the point of tangency would fall at T_{SP}. A muscle almost entirely unable to sideslip because of intermuscular membranes would remain on the "primary position path" through most of its contact with the globe, leaving, perhaps, at T_{PP}. The actual muscle path lies between these two extremes, as does the actual point of tangency T_{AP}.

tact. These fascial "springs" tend to hold the muscle to its primary position path and reduce globe-relative sideslip. As the eye rotates out of primary position the muscle may (depending on the direction of rotation and the muscle tension) be pulled sideways off its primary position path. Since only the point of tangency (and not the precise shape of the path from insertion to point of tangency) is mechanically important, we assumed a simple circular shape for the arc of contact. From each muscle's force and the geometry of its path, we compute the force tending to slip the muscle sideways on the globe. We suppose that the fascial springs stiffen as they stretch according to a two-parameter exponential equation (Miller and Robinson, 1984, equation 15).

Although there is extensive data describing the fixed orbital contents, based on dissection and serial sectioning of cadaver orbits (Volkman, 1869; Nakagawa, 1965; Koornneef, 1983), the need for descriptions with the eye in various gaze positions has not been widely recognized. Our modeling efforts have made this need apparent. It might be thought that these data could be obtained by manipulation of fresh cadaver orbits. However, muscle paths depend on muscle tension (Miller and Robinson, 1984), and such data can only be obtained from an awake subject executing voluntary eye movements.

The purpose of this study, then, was to provide some data on the paths of extraocular muscles in a physiologic situation. Specifically, we sought to visualize the lateral rectus muscle as a trained monkey fixed various known positions.

It is useful to measure sideslip in two reference frames:

(1) As sideways movement of the point of tangency T relative to the *orbit*. If T were fixed in the orbit, for instance, each muscle plane would be fixed as well. The intuitive understanding of muscle action would be greatly simplified. (This assumes that globe translations are small, and that the path from T to the origin O does not change shape.) Also, neural control eye position might be simplified if muscle actions did not change with eye position.

(2) As sideways movement of the point of tangency T relative to the *globe*. Orbital anatomy suggests that fascial connections mainly couple each muscle to the globe, rather than to the orbit. The elasticity of these connections, therefore, should be strongly related to globe-relative displacement (see Miller and Robinson, 1984).

In order to analyze the data of the present study, certain aspects of monkey orbital geometry must be known. However, we will obtain a more complete description than is necessary for this purpose, because of its general value in computer modeling studies of monkey orbital statics.

METHODS

Subjects and preparation

Two male juvenile monkeys were used in the X-ray studies: one *M. radiata* and one *M. fascicularis*.

Under aseptic conditions and surgical anesthesia, each monkey was fitted with a head plate, and a scleral search coil. The coil was implanted in the right eye using a method that does not tend to induce strabismus (Judge *et al.*, 1980).

Taking care to minimize damage to intermuscular membranes, radio-opaque markers were implanted in the left lateral rectus of each monkey. In one monkey (the *M. fascicularis*) we tied knots using 5-0 multifilament stainless steel suture. In the other (the *M. radiata*) we implanted fine lead wire. The superior and inferior margins of the muscle were marked at the insertion and at several points posterior, as far back into the orbit as could be reached without having to dissect the muscle from its attachments. The two markers at the insertion served as reference points on the globe, and the remaining markers to delineate the muscle path. It would have been convenient to implant additional markers in the globe, specifically, under the belly of the LR, but this could not be done without significant damage to the intermuscular membranes. Sutures under the muscle would also be expected to cause scarring between the globe and the muscle. Either of these artifacts might have seriously affected the results.

When healing was complete, the monkeys were trained to fix red LED's at each of 9 "diagnostic positions of gaze" in a square ± 25 deg horizontally and vertically.

X-ray images

By visual inspection of the corneal reflex (Hirshberg test) we determined that each

monkey was orthophoric. (This method would be expected to detect misalignments as small as about 5 deg.) A portable X-ray machine was positioned 183 cm in front of the marked left lateral rectus muscle, with the skull in lateral view. An X-ray film cassette was placed so that the film was 2.5 cm behind the marked muscle, allowing the resulting X-ray image to be considered a parallel projection into the sagittal plane. A notched metal strip was placed in the plane of the marked muscle to calibrate length measurements in the X-ray image. Each LED was lit in turn, and an X-ray exposure taken while the monkey held fixation, as verified by means of the search coil in the right eye. If fixation was lost around the time of an X-ray exposure, the exposure was repeated.

Orbital geometry

Four eyes of juvenile monkeys (one *M. radiata* and three *M. mulata*) were dissected and measured in a stereotaxic instrument.

The heads were mounted in the usual way with ear-bars, and an orbital rim and palate clamp. The roof and temporal wall of the orbit were carefully removed using a bone saw and rongeurs. The globe was injected with normal saline, as needed, to retain its shape. A stiff wire pointer was attached to a three-axis micromanipulator on a carriage, which rode on the stereotaxic rails. This pointer was used to measure the coordinates of the origins and insertions of the muscles, and of points on the surface of the globe. Muscle and tendon lengths were determined with the tissues hydrated with normal saline and laid flat on a glass surface. Muscle cross-sections were estimated by weighing each muscle (without the tendon) and dividing by the product of its length and the density of muscle tissue (1 g/cm^3).

Calculation of sideslip

Sideslip was calculated as the sideways movement of the point of tangency T (1) relative to the *orbit*, and (2) relative to the *globe*.

T was the mechanically important point for determining muscle action. Therefore, we measured sideslip as the sideways movement of T rather than of some fixed point on the muscle (a different point on the muscle was tangent to the globe in different eye positions). We calculated orbit-relative sideslip first, and from it, calculated globe-relative sideslip.

Figure 3(A) shows the measurement of orbit-relative sideslip.

(1) The midpoint of the line joining the two insertional sutures was taken as the "point insertion" R; its projection in the plane of the X-ray was called [R]. A curve was hand-drawn from [R] down the middle of the muscle, using the 2 rows of sutures as a guide. The projected point of tangency [T] fell on this curve.

(2) To find the projected point of tangency [T] on this curve, we assumed that the muscle took a straight path from its origin to T, and that the globe was a sphere that rotated about its center. From the mean globe radius, and the coordinates of the origin and insertion of the LR (Table 1), we calculated that [T] fell 8.4 mm posterior to [R], for primary position gaze [Fig. 3(B)].

(3) The anterior-posterior location of [T] would have been independent of gaze and sideslip if the plane of the X-ray had been parallel to the axis of the orbital cone (we would have been looking "edge-on" at the circle of tangency of the LR with the globe; see Fig. 2). However, the X-ray image was sagittal, so that the horizontal location of [T] was a function of orbit-relative sideslip. (As the muscle slipped upwards, for instance, [T] moved anteriorly.) Because orbit-relative sideslip was small, and the image of the posterior portion of the marked muscle (more precisely, the line segments joining the bisectors of the noninsertional suture pairs) was close to horizontal in all gaze positions, this effect was very small. For instance, if [T] moved 3 mm upwards, it would have also moved 0.3 mm anterior. With respect to the vertical position of [T] calculated in paragraph "2", above, this would produce an error of less than 0.05 mm. We considered this negligible.

(4) The head restraint was sharply defined in the X-ray and provided convenient landmarks for constructing the orbital reference. Figure 3(A) shows the line we used as the orbital reference. In each X-ray we measured the perpendicular distance from [T] to this line.

(5) When the eye was in primary position, we took sideslip to be zero. Subtracting this distance from each of the 9 measurements gave the "projected orbit-relative sideslip" values. Because the magnitude of orbit-relative LR sideslip was small, projection distortion was negligible.

To transform orbit-relative sideslip, calculated above, to globe-relative sideslip, we found the vector **t** describing point T in an orbit-fixed Cartesian coordinate system with the origin at the center of rotation. The coordinate trans-

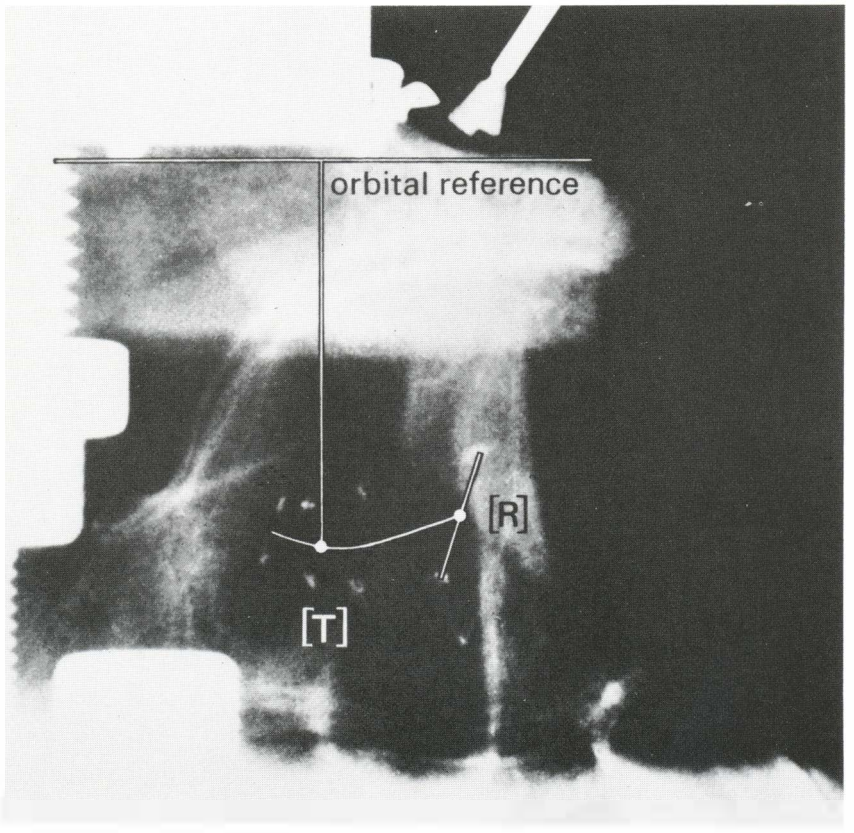

(A)

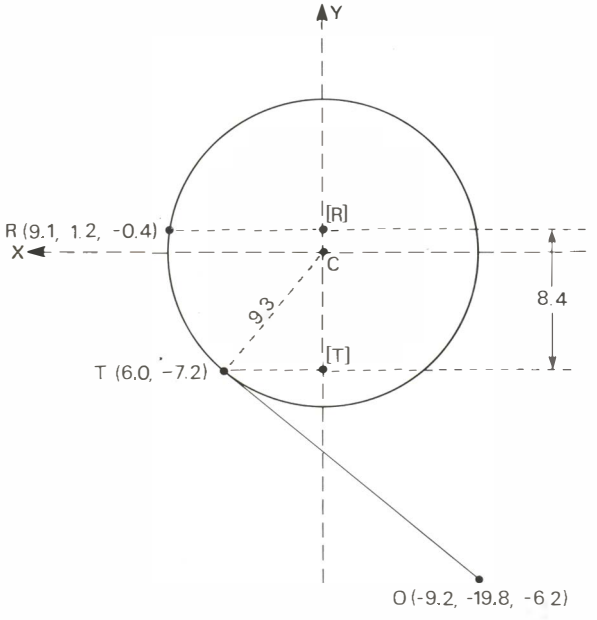

(B)

Fig. 3. Measuring orbit-relative sideslip. (A) In this X-ray image of the eye in primary position, the 2 rows of implanted sutures can be seen as small white knots. The two insertional sutures are connected by a short, straight construction line, the center of which is the projection of the insertion [R]. The curved construction line marks the middle of the muscle, along which the projected point of tangency [T] is found (see text). The orbital reference is a horizontal line, drawn with reference to the head restraint. The search coil used to measure eye position can be seen just anterior to the insertional sutures. (B) A horizontal section through the left eye and lateral rectus is shown schematically, as viewed from above, with the eye in primary position. Coordinates of the origin O and insertion R, as well as the mean globe radius, are taken from Table 1. The projections into the plane of the X-ray image of the insertion [R] and the point of tangency [T] are separated horizontally by 8.4 mm.

formation for a Fick coordinate system is given by

$$\mathbb{A} = \begin{bmatrix} \cos\theta\cdot\cos\psi & \sin\phi\cdot\sin\theta & \sin\psi\cdot\cos\theta \\ +\sin\psi\cdot\sin\phi\cdot\sin\theta & & -\sin\theta\cdot\cos\psi\cdot\sin\phi \\ \sin\psi\cdot\sin\phi\cdot\cos\theta & \cos\phi\cdot\cos\theta & -\sin\psi\cdot\sin\theta \\ -\sin\theta\cdot\cos\psi & & -\cos\theta\cdot\cos\psi\cdot\sin\phi \\ -\sin\psi\cdot\cos\phi & \sin\phi & \cos\psi\cdot\cos\phi \end{bmatrix}, \quad (1)$$

where θ, ϕ, and ψ are the horizontal, vertical, and torsional components of eye position. Denoting the transformed values with primes, we have

$$\mathbf{t}' = \mathbb{A}^{-1}\cdot\mathbf{t}. \quad (2)$$

The z' component of $\mathbf{t}'$ was taken as "sideslip relative to the globe".

Adjustment for scarring

As we expected, the implanted sutures and the surgical procedure itself caused some scarring. To evaluate the effect of this on sideslip, we measured the sideslip stiffness of an LR with implanted sutures, and compared it to the stiffness of the fellow LR, which had not been previously disturbed.

We could not use an animal with an implanted search coil for this purpose, since it would not have an undisturbed LR for comparison. We, therefore, prepared an *M. mulata* with EOG electrodes implanted in the periorbital bone, planning to run it in the main experiment as well. Unfortunately, instability of the electrodes made this latter impossible. Therefore, this animal was used only for measurement of sideslip stiffness. The stiffness measurements were made just prior to sacrificing the animal, under deep pentobarbitol anesthesia.

(1) A bilateral lateral orbitotomy was performed, disturbing the orbital contents as little as possible.

(2) With each eye held in primary position with forceps, a suture was tied around the LR at its point of tangency, as determined visually.

(3) With the eye still held in primary position, each suture was grasped with ultrasonic length-tension forceps (Collins, 1976), and the stiffness to sideways movement was measured by making several pulls superiorly and inferiorly. This instrument was calibrated to an accuracy of $\pm 1\%$ in force and $\pm 3\%$ in displacement. Misalignment of the forceps would result in underestimation of stiffness, however, they are not sensitive to small misalignments and, unlike the case in which these forceps are used to measure *rotational* stiffness of the eye, proper alignment was easy to maintain.

(4) Offsets in force and displacement, from one "pull" to the next, are not well controlled with hand-held length-tension forceps. There-

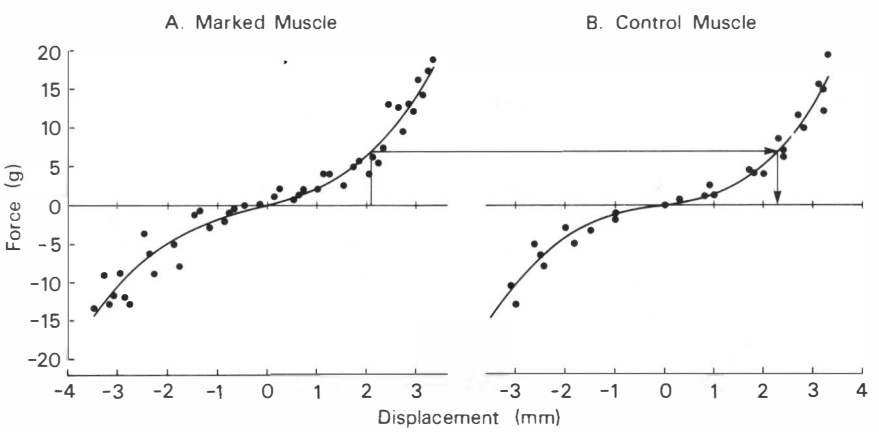

Fig. 4. LR sideslip stiffness. Individual data points are shown along with best-fitting 3rd-order polynomial curves. Data sets resulting from each "pull" were adjusted to align the inflection points before the curve was fitted. (A) Marked muscle; data from 6 pulls ($r = 0.98$). (B) Control muscle; data from 3 pulls ($r = 0.98$).

fore, for each of the experimental and control data sets, the data from multiple pulls were aligned by making their points of inflection coincide, and a third-order polynomial was fitted. Figure 4(A) shows the stiffness of the LR marked with stainless steel sutures, and Fig. 4(B) that of the LR in the eye not previously disturbed. Comparison of Fig. 4(A) and (B) shows that the surgery stiffened the intermuscular tissues slightly.

(5) To correct for this surgical artifact, the sideslipping force was found from Fig. 4(A) for each globe-relative sideslip (displacement) value computed above. Then, using Fig. 4(B), the displacement of a normal muscle was found for that force. (This calculation is indicated in Fig. 4.) These corrected globe-relative sideslip values are given in Table 3.

(6) These corrections to the position of T in space were directly applied to the orbit-relative sideslip values. These are given in Table 4.

RESULTS

Monkey orbital geometry

Table 1 gives the mean values of the orbital parameters we measured, along with their standard deviations (σ_{n-1}).

Differences between measurements on the two species (*M. radiata* and *M. mulata*) were not greater than within-species differences. However, since no *M. fascicularis* eyes were measured, generalization of the results to this species is uncertain.

We are less confident of certain values in Table 1 than of others. The insertions of the IR and IO were difficult to visualize without moving the globe and, thus, disturbing the measurement. The standard deviations of these values tend to reflect this difficulty. Secondly, the separation of muscle from tendon was somewhat arbitrary, since the fleshy tissue does not always end sharply. The sum of muscle length

Table 1. Monkey ocular geometry

Parameter		Muscle LR	MR	SR	IR	SO	IO
Origin (mm)							
	X	−9.2 (0.6)	−12.0 (1.3)	−10.8 (1.9)	−11.2 (1.1)	−9.7 (1.3)	−5.8 (1.3)
	Y	−19.8 (1.2)	−19.6 (2.6)	−19.4 (1.0)	−18.6 (1.6)	7.5 (2.7)	5.2 (1.4)
	Z	−6.2 (0.9)	−5.6 (1.1)	−4.0 (1.4)	−8.1 (0.2)	6.8 (0.8)	−11.6 (1.1)
Insertion (mm)							
	X	9.1 (0.5)	−9.4 (0.7)	2.1 (1.0)	1.4 (1.9)	1.6 (0.9)	3.4 (3.8)
	Y	1.2 (0.8)	2.6 (1.2)	2.0 (0.4)	3.1 (1.6)	−4.3 (0.7)	−7.8 (0.9)
	Z	−0.4 (1.0)	0.1 (0.3)	8.2 (0.6)	−8.3 (0.6)	8.2 (0.5)	−0.8 (1.7)
Direct length (mm)						25.8 (1.7)	
Muscle length (mm)		17.7 (0.4)	19.0 (2.1)	19.9 (2.8)	18.9 (2.2)	15.7 (2.1)	17.3 (2.6)
Adjusted muscle length (mm)		19.7	20.0	21.9	17.9	15.0	18.5
Tendon length (mm)		7.0 (2.8)	0.5 (0.7)	4.0 (0.5)	5.0 (1.4)	25.8 (4.3)	0.0 (0.0)
Muscle width at insert (mm)		5.9 (1.1)	6.2 (1.9)	5.0 (1.2)	4.5 (1.0)	4.9 (1.2)	6.2 (2.2)
Muscle cross section (mm^2)		10.4 (0.5)	8.9 (1.8)	6.1 (0.5)	7.8 (1.4)	4.8 (0.6)	6.3 (0.8)
Mean globe radius (mm)	9.3 (0.5)						

Values are derived from quantitative dissection of 4 monkey eyes: 1 *M. radiata* and 3 *M. mulatas*. Below each mean value is the standard deviation (σ_{n-1}) in parentheses. For each muscle (LR, MR, SR, IR, SO, and IO) the positions of the *origin* and *insertion* are given in the Cartesian coordinate system of Fig. 1. For the SO, the mechanically-effective origin (at the trochlea) and the distance between the trochlea and the anatomic origin (*direct length*) are given. *Muscle length* is exclusive of tendon. *Adjusted muscle length* is derived from muscle length, as explained in the text. *Muscle cross section* is the weight of the muscle (without tendon) divided by the product of its length and density.

Table 2. Muscle unit moment vectors in primary position

Species	Component	Muscle LR	MR	SR	IR	SO	IO
Monkey	m_x (depression)	0.09	0.06	−0.88	0.87	0.71	−0.88
	m_y (intorsion)	−0.33	0.24	0.46	−0.50	0.67	−0.41
	m_z (abduction)	0.94	−0.97	0.11	−0.04	0.22	0.24
Human	m_x (depression)	−0.02	−0.01	−0.87	0.85	0.59	−0.63
	m_y (intorsion)	0.02	−0.01	0.41	−0.41	0.79	−0.76
	m_z (abduction)	1.00	−1.00	−0.29	−0.32	0.16	−0.14

The components of **m** are given in the coordinate system of Fig. 1, as calculated from the data of Table 1 for the monkey, and from the data given by Miller and Robinson (1984, Table 1) for the human.

and tendon length is probably more reliable than either value separately. Finally, our calculation of muscle cross-section is somewhat arbitrary. Instead of measuring mean cross-section, for instance, we might have measured maximum cross-section. It is not clear which is the best measure of muscle strength.

If we replace each pair of tendon and muscle length measurements with its sum, then (except for a weak dependence of the muscle cross-section measurement on the muscle length measurement), the values in Table 1 are independent of each other. It is therefore possible that, because of experimental error, these values are not consistent. To find out, we calculated the degree of stretch of each muscle in primary position, given the geometry implied by Table 1. We took account of the globe translation that must be expected when the muscles are innervated, which the SQUINT model predicts to be 0.27 mm nasally and 0.19 mm inferiorly. We reasoned that stretch, as a fraction of resting muscle length, would be similar for all the muscles, since muscle tissue tends to elongate or shorten if chronically stretched or slackened, respectively (Goldspink, 1985; Williams and Goldspink, 1984). The model showed primary position stretches from 5% (for the IR) to 24% (for the LR). We chose to adjust the "muscle length" values to force consistency, and did so to produce 10–12% stretch in each muscle in primary position. The resulting "adjusted muscle length" values are given in Table 1. In no case do they differ more than 2 mm from the measured values.

The unit moment vector **m** for the monkey eye in primary position may be calculated for each muscle from the data of Table 1. These values are given in Table 2, along with the comparable values for the human eye, based on the human anatomic data given in Miller and Robinson (1984).

Unit moment vectors for the eye in primary position were calculated as the negative (because of the left-handed coordinate system) cross product of the vector from C to R with that from C to O (see Fig. 1). Globe translation caused by muscle forces was taken into account for the monkey as described above, and for the human (translations of 0.41 mm nasally and 0.43 mm posteriorly).

Sideslip relative to the globe

The mean values of globe-relative sideslip are given in Table 3. On average, a vertical eye

Table 3. Sideslip relative to the globe

		AD −25°	0°	AB +25°
Up	+25°	2.2 (0.1)	2.4 (0.4)	2.8 (1.1)
	0°	−1.3 (0.0)	0.0	1.3 (1.3)
Down	−25°	−3.4 (0.4)	−2.7 (0.6)	−1.8 (1.2)

Values are derived from two monkeys: 1 *M. radiata* and 1 *M. fascicularis*. Below each mean value is the standard deviation (σ_{n-1}) in parentheses. Positive sideslip is upward; negative downward (mm). The nine sideslip values are for the nine gaze positions shown (deg). Sideslip in primary position is taken to be 0.

Table 4. Sideslip relative to the orbit

		AD −25°	0°	AB +25°
Up	+25°	−1.6 (0.2)	−0.8 (0.5)	0.3 (1.2)
	0°	−1.3 (0.0)	0.0	1.3 (1.3)
Down	−25°	0.2 (0.4)	0.5 (0.6)	0.9 (1.3)

Values are derived from two monkeys: 1 *M. radiata* and 1 *M. fascicularis*. Below each mean value is the standard deviation (σ_{n-1}) in parentheses. Positive sideslip is upward; negative downward (mm). The nine sideslip values are for the nine gaze positions shown (deg). Sideslip in primary position is taken to be 0.

movement from −25 to +25 deg is accompanied by 5.1 mm of vertical sideslip relative to the globe ($t[1] = 48.1$; $P < 0.01$, 1-tail). Sideslip is greatest (5.6 mm) if the eye moves from depression to elevation in adduction, less (5.1 mm) if it moves from straight down to straight up, and least (4.6 mm) if it elevates in abduction. The dependence of globe-relative sideslip on horizontal eye position is weak, but statistically significant ($F[2,2] = 121.0$; $P < 0.01$). The differences between sideslip on elevation compared to depression are not consistent.

We can compare these measurements with the sideslip expected on the basis of the "shortest path" hypothesis (see Fig. 2). In abduction we would expect 3.4 mm of vertical sideslip, which is not significantly different from the 4.6 mm we measured. As the eye moves straight up and down we would expect 5.0 mm of sideslip, also not significantly different from the 5.1 mm measured. In adduction, however, when the arc of contact of the LR with the globe is large, the shortest path hypothesis predicts 7.3 mm of sideslip, while we measure only 5.6 mm ($t[1] = 12.36$; $P < 0.05$, 1-tail).

Sideslip relative to the orbit

The mean values of orbit-relative sideslip are given in Table 4. It can be seen that in elevation the point of tangency moves down slightly, while in depression (in 2 out of 3 cases) it moves up. This perhaps unexpected direction of movement will be discussed below. Summing across horizontal eye positions, mean orbit-relative sideslip of −1.2 mm was measured ($t[1] = 12.2$; $P < 0.05$, 1-tail).

The main point to notice about orbit-relative sideslip, however, is that it is minimal: no more than 1.8 mm for a 50 deg vertical movement.

CONCLUSIONS

Stability of muscle planes

Our results show that the point of tangency T of the LR does not move much in a vertical direction, relative to the orbit. If the center of rotation of the globe is assumed fixed, this implies that all 3 coordinates of T are approximately stationary in the orbit, and that the unit moment vector **m** is approximately fixed as well.

This conclusion supports the usefulness (at least for roughly understanding muscle actions) of the notion that muscle planes are fixed in the orbit (e.g. Scott, 1983). Thus, for instance, as the eye elevates, one can appreciate that the LR develops an intorting action (simply because of the reorientation of the visual axis, about which torsion is defined), without the complication of considering an emergent vertical action.

The cooperative action that a pair of antagonistic muscles might develop in certain gaze positions is called a "bridle effect" (Robinson, 1975). For example, the horizontal recti might become elevators in upgaze (or depressors in downgaze). This would occur because their points of tangency T had slipped up (or down) relative to the orbit. The existence of a bridle effect would seem to make the brainstem's task of oculomotor control very difficult, leading some to propose that other effects cancel it. France and Burbank (1979) for instance, suggest that the nonuniform distribution of tension across the width of the muscle displaces the effective insertion enough to cancel the bridle force. The present results suggest that there is no bridle force to cancel.

Although we must be cautious in generalizing this finding to humans and to muscles other than the LR, Simonsz (1985) has found supporting evidence in human CT scans that all four recti remain approximately fixed in orbit.

There is no evidence concerning the stability of the planes of the oblique muscles.

Muscle actions

The geometric data of Table 1 are substantially different from the comparable human data (see, e.g. Miller and Robinson, 1984).

If we take the mean origin of the rectus muscles to define the orbital apex, we can make the following calculations. Although the diameter of the monkey globe is 75% that of the human, the distance between the globe center and the orbital apex is only 65% that of the human, making the monkey orbit relatively shorter. The monkey orbital axis points 28 deg outward compared to 26 deg outward in the human, and 15 deg upward compared to 1 deg downward in the human. The angular arcs of contact of the muscles with the globe in primary position are quite different. Mechanically, the most important difference is that the monkey medial rectus has only a 9 deg arc of contact, compared to 35 deg in the human. Nevertheless, monkeys have at least a ±40 deg oculomotor range (horizontally and vertically), and it is something of a mystery how the MR, a muscle of moderate cross-section, can lose tangency at

9 deg of adduction and still adduct the eye so effectively.

The differences between the geometry of monkey and human eyes are sufficient to produce some qualitative differences in primary position muscle actions. Each component of **m** given in the Table 2 may be understood as the fraction of the muscle's force acting about the component axis. Thus, it is seen that monkey horizontal recti have a substantial torsional action (m_y), while human horizontal recti do not. Monkey vertical recti lack the adducting action found in the human (m_z). Finally, m_x is larger in absolute value than m_y for both the superior and inferior obliques in monkey. This means that for a monkey eye in primary position, the obliques have more vertical than torsional action.

Mechanical determinants of sideslip

Sideslip is determined by (1) muscle tension, (2) forces exerted by intermuscular attachments, and (3) forces exerted by muscular-orbital attachments. The SQUINT model assumes the last of these to be negligible. Koornneef (see Koornneef, 1983), however, has carefully sectioned fixed human orbits to demonstrate the existence of fascial sheets connecting the muscles with the bony orbit as well as with each other. If the muscular–orbital coupling were stiffer than the intermuscular coupling, it might explain our observation that the LR point of tangency tends to be stationary with respect to the orbit. Unfortunately, Koornneef's studies were purely anatomical and do not describe the mechanical properties of the various fascial sheets. Observations during our monkey dissections and during human strabismus surgery, however, suggest that the major coupling is intermusclar. Also, if muscular–orbital coupling was dominant, the tendency of T to move up with respect to the orbit as the eye looks down, and down as the eye moves up, would be hard to explain. That is, muscle tension would tend to make the muscle take the shortest path, and muscular–orbital attachments could only reduce, but not reverse, this tendency.

We propose, then, to explain our results as due to the sum of two forces: (1) muscle tension, and (2) the forces exerted by intermuscular attachments.

Muscle tension tends to cause the muscle to sideslip relative to the globe. In elevation, for example, the LR tends to slip upward, toward the shortest path across the globe. Intermuscular attachments, on the other hand, tend to reduce globe-relative sideslip by effectively coupling the muscles to the globe. Because T lies posterior to the center of rotation [see Figs 2 and 3(B)], it is possible for T to move opposite to the direction of rotation. In elevation, for example, T tends to move down (see Table 4).

Perhaps, then, the relative stability of T with respect to the orbit is due to the balancing of these two forces. Coupling of the muscles to the orbit might further stabilize them.

Acknowledgements—The authors thank Drs Edward Keller and William Crandall for the use of their animal surgical and testing facilities, Mr Charles Clay and his staff at the Pacific Presbyterian Medical Center Department of Radiology for the X-ray images, and Dr Alan Scott for his help with ocular surgery. This study was supported by Grant EY04565 from the National Eye Institute, National Institute of Health, Bethesda, Maryland, and by the Smith-Kettlewell Eye Research Foundation.

REFERENCES

Boeder P. (1962) Co-operative action of extraocular muscles. *Br. J. Ophthal.* **46,** 397–403.

Collins C. C. (1976) Length-tension recording strabismus forceps. In *Smith-Kettlewell Symposium on Basic Sciences in Strabismus. Proceedings of the V Congress (Annex) of the Conselho Latino-Americano de Estrabismo*, Guaruja, Brazil, pp. 7–19.

Collins C. C., Carlson M., Scott A. B. and Jampolsky A. (1981) Extraocular muscle forces in normal human subjects. *Invest. Ophthal. visual Sci.* **20,** 652–664.

Collins C. C., Scott A. B. and O'Meara D. M. (1969) Elements of the peripheral oculomotor apparatus. *Am. J. Optom.* **46,** 510–515.

France T. D. and Burbank D. P. (1979) Clinical applications of a computer-assisted eye model. *Trans. Am. Acad. Ophthal. Otolar.* **86,** 1407–1412.

Goldspink G. (1985) Malleability of the motor system: a comparative approach. *J. exp. Biol.* **115,** 375–391.

Judge S. J., Richmond B. J. and Chu F. C. (1980) Implantation of magnetic search coils for measurement of eye position: an improved method. *Vision Res.* **20,** 535–538.

Koornneef L. (1983) *Orbital Connective Tissue*. Chap. 32 in Vol. 1 of Duane T. D. and Jaeger E. A. *Biomedical Foundations of Ophthalmology*. Harper & Row, Philadelphia, Pa.

Krewson W. E. (1950) The action of the extraocular muscles; a method of vector analysis with computations. *Trans. Am. ophthal. Soc.* **48,** 443–486.

Miller J. M. and Robinson D. A. (1984) A model of the mechanics of binocular alignment. *Comput. Biomed. Res.* **17,** 436–470.

Nakagawa T. (1965) Topographic anatomical studies on the orbit and its contents. *Acta soc. ophth. jap.* **69,** 2155–2179.

Robinson D. A. (1975) A quantitative analysis of extraocular muscle cooperation and squint. *Invest. Ophthal.* **14,** 801–825.

Robinson D. A., O'Meara D. M., Scott A. B. *et al.* (1969)

Mechanical components of human eye movements. *J. appl. Physiol.* **26,** 548–553.

Scott A. B. (1983) Ocular motility. In *Biomedical Foundations of Ophthalmology*, Chap. 23. Harper & Row, Philadelphia, Pa.

Simonsz H. J., Harting F., de Wall B. J. and Verbeeten B. W. (1985) Sideways displacement and curved path of recti eye muscles. *Archs Ophthal.* **103,** 124–128.

Volkmann A. W. (1869) On the mechanics of the eye muscles. *Ber. Verh. Sachs. Ges. Wsch.* **21,** 28–69.

Williams P. E. and Goldspink G. (1984) Connective tissue changes in immobilised muscle. *J. Anat.* **138,** 343–350.